

Blind spheres of paramagnetic dopants in solid state NMR

Wenyu Li^[a], Qianyun Zhang^[a], Jonas J. Joos^[b], Philippe F. Smet^[b], Jörn Schmedt auf der Günne^{*,[a]}

[a] Inorganic Materials Chemistry, University of Siegen, Adolf-Reichwein-Str. 2, 57076 Siegen, Germany

[b] LumiLab, Department of Solid State Sciences, Ghent University, Krijgslaan 281-S1, 9000 Gent, Belgium.

*gunnej@chemie.uni-siegen.de

Supporting information

1. Line width and isotropic chemical shift changes of $\text{La}_{1-x}\text{Sm}_x\text{PO}_4$ series

In order to test whether the Sm^{3+} NMR data would show correlations to the doping level x , both the isotropic chemical shift values (δ_{iso}) and the line width ($\Delta\nu$) for three different environments have been plotted against x (Fig. S1). The three components are: (1) the comparably sharp signal at the LaPO_4 signal position of around -4.6 ppm, (2) the comparably broad signal whose $\delta_{\text{iso}} > 0$ ppm and shifts towards the SmPO_4 signal position as x increases, (3) the signal in between the previous two signals. When $x > 0.1$, peaks can't be well separated due to the overlap of different components. Nevertheless, positive correlations could be rationalized between δ_{iso} , $\Delta\nu$ and x , although the overlap would introduce large data scattering for deconvolution. In order to present the correlation as well as indicate the large data scattering, data points with same x were plotted, which were obtained by deconvolution from different starting values on the same spectrum.

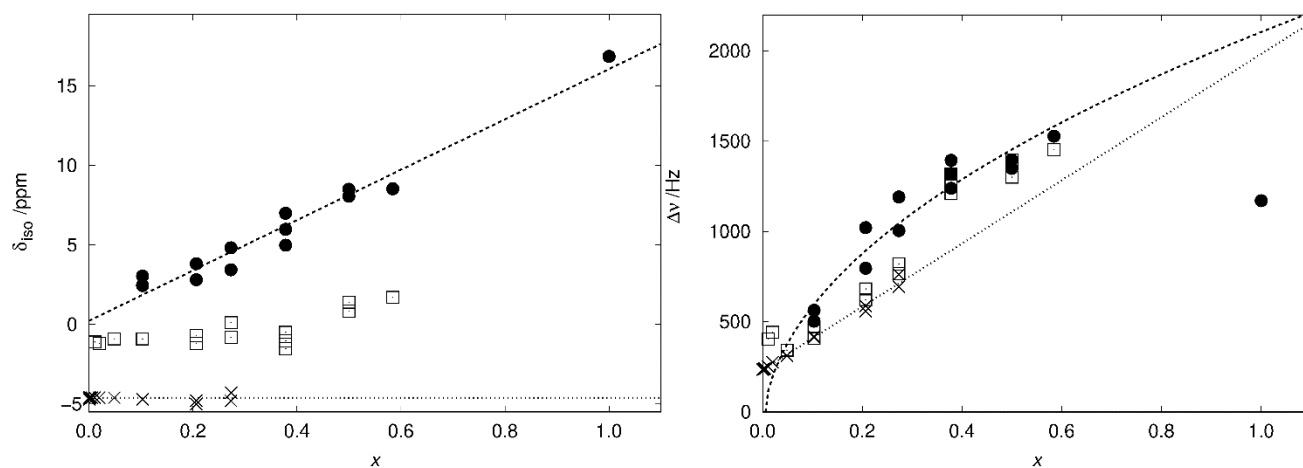


Figure S1: (left) isotropic chemical shift values as a function of the substitution degree x in 1000 °C co-precipitated $\text{La}_{1-x}\text{Sm}_x\text{PO}_4$, the dashed line represents linear fits resulting in $\bar{\delta}_{\text{iso}}/\text{ppm} = 0.2 + 15.8 \cdot x$, and the dotted lines represent $\bar{\delta}_{\text{iso}}/\text{ppm} = -4.6$. (right) line width as a function of the substitution degree x in co-precipitated $\text{La}_{1-x}\text{Sm}_x\text{PO}_4$, the dashed line represent $\Delta\nu/\text{Hz} = -115 + 2220 \cdot x^{1/2}$, and the dotted line represents $\Delta\nu/\text{Hz} = 234 + 1749 \cdot x$. The data points of the same x show significant scattering of the fitted parameters for overlapping signals.

A linear relation only holds for the peak component (Fig. S1 crosses) at around -4.6 ppm, which is close to the ^{31}P shift for non-doped diamagnetic LaPO_4 . For the broad component (Fig. S1 circles) which stretches further towards SmPO_4 signal as x increases, a linear relation, which was suggested earlier in literature^{1,2}, is not describing the experimental data well. A square root function provides a more reasonable fit. As for the middle component (Fig. S1 squares), which lies in between two previously peaks, the functional dependence is more difficult to identify and needs more components.

2. Exchange 2D spectra for $\text{La}_{1-x}\text{Ln}_x\text{PO}_4$ (Ln = Nd, Dy, Ho, Er, Tm, Yb)

2D exchange spectroscopy (EXSY) ^{31}P MAS experiments with zero mixing time show a sharp ridge on the diagonal (Fig. S2) for $\text{La}_{1-x}\text{Ln}_x\text{PO}_4$ (Ln = Nd, Dy, Ho, Er, Tm, Yb) samples, which is typical for inhomogeneous broadening.

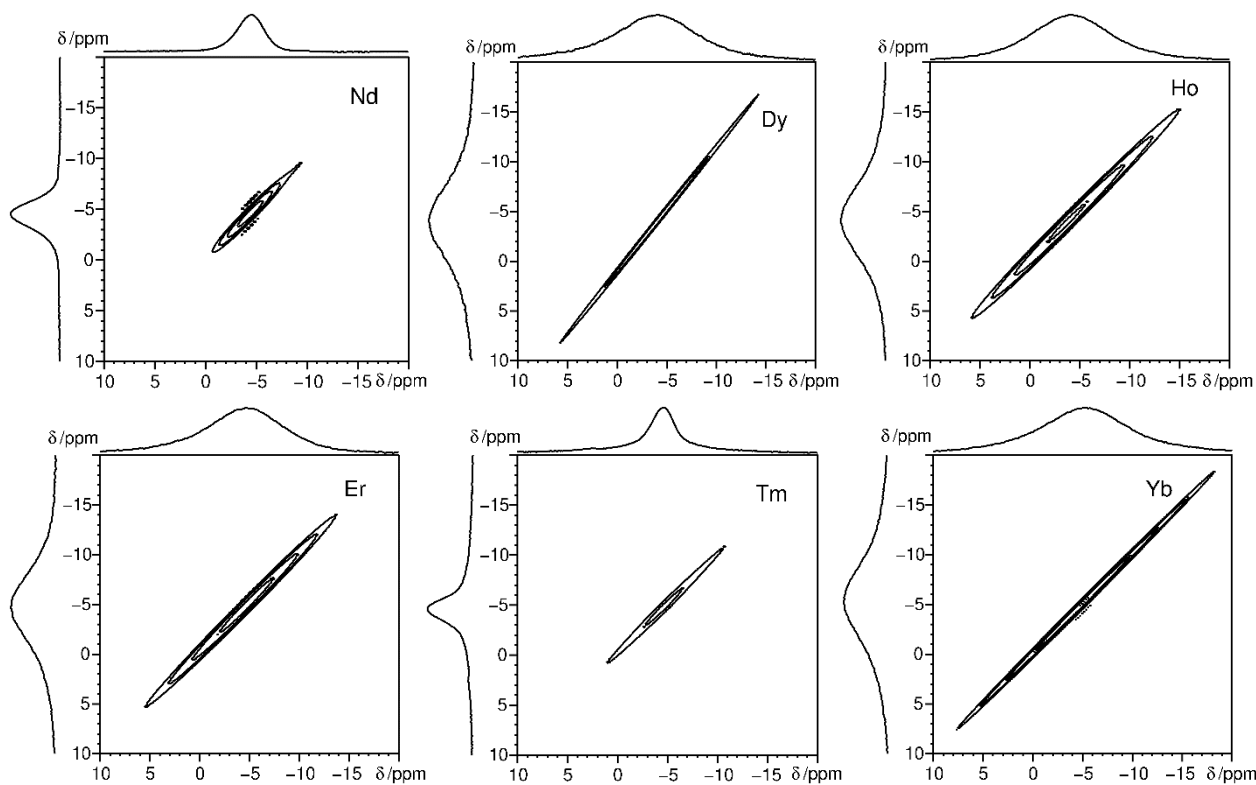


Figure S2: 2D ^{31}P MAS EXSY spectra (with zero mixing time) for $\text{La}_{0.98}\text{Nd}_{0.02}\text{PO}_4$, $\text{La}_{0.995}\text{Dy}_{0.005}\text{PO}_4$, $\text{La}_{0.99}\text{Ho}_{0.01}\text{PO}_4$, $\text{La}_{0.99}\text{Er}_{0.01}\text{PO}_4$, $\text{La}_{0.995}\text{Tm}_{0.005}\text{PO}_4$ and $\text{La}_{0.98}\text{Yb}_{0.02}\text{PO}_4$, which all show a lineshape consistent with inhomogeneous line broadening. MAS spinning frequency is 10 kHz for $\text{La}_{1-x}\text{Ln}_x\text{PO}_4$ $\text{Ln} = \text{Nd}, \text{Dy}, \text{Tm}$ and 12.5 kHz for $\text{Ln} = \text{Ho}, \text{Er}, \text{Yb}$.

3. Different correlations blind sphere radius with Ln-parameters

The factor $C_{\text{SA}} = g^2 J(J+1)^4$ refers to the lanthanide free-ion and gives indication on the size of the anisotropy shielding contribution to hyperfine shift. The parameter C_{con} refers to the size of electronic contribution from contact shielding⁴. The blind sphere sizes r_0 of measured lanthanide ions were plotted against both $\sqrt[3]{|C_{\text{SA}}|}$ (Fig. S3) and $\sqrt[3]{|C_{\text{con}}|}$ (Fig. S4). A linear dependence $r_0 \propto \sqrt[3]{|C_{\text{SA}}|}$ was observed (Fig. S3) except for Gd^{3+} . Such correlation indicates that, for the same host, treating the dopant ions as free lanthanide ions provides a reasonable estimate of the trend of the size of the blind sphere. Also contact and pseudo-contact contributions were considered. An empirical linear dependence $r_0 \propto \sqrt[3]{|C_{\text{con}}|}$ was observed (Fig. S4) for all Ln^{3+} including Gd^{3+} .

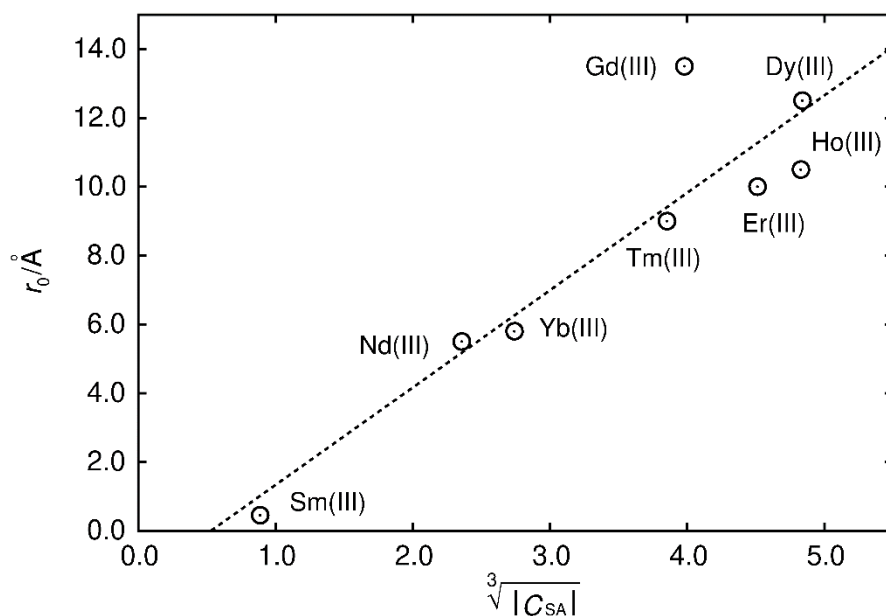


Figure S3: Blind sphere radii for Ln(III) dopants of $\text{La}_{1-x}\text{Ln}_x\text{PO}_4$ series, plotted against $\sqrt[3]{|C_{SA}|}$. $|C_{SA}|$ refers to the magnitude of hyperfine contribution from anisotropy shielding⁴. The dashed line features the fitting function $r_0/\text{\AA} = -1.50 + 2.83 \cdot \sqrt[3]{|C_{SA}|}$ with $R^2 = 0.85$.

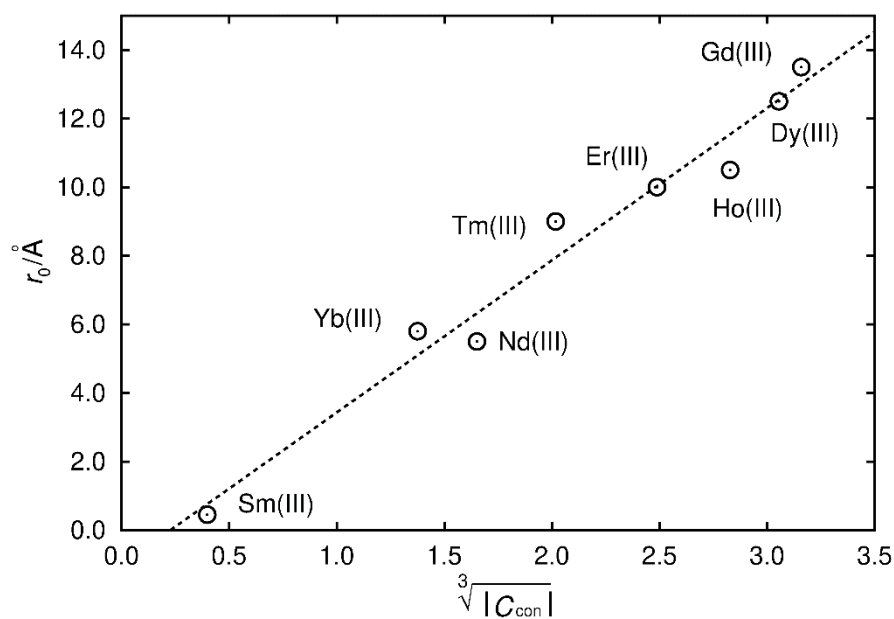


Figure S4: Blind sphere radii for Ln(III) dopants of $\text{La}_{1-x}\text{Ln}_x\text{PO}_4$ series, plotted against $\sqrt[3]{|C_{con}|}$. $|C_{con}|$ refers to the magnitude of electronic contribution from contact shielding⁴. The dashed line features the fitting function $r_0/\text{\AA} = -1.01 + 4.44 \cdot \sqrt[3]{|C_{con}|}$ with the coefficient of determination $R^2 = 0.97$.

4. ^{31}P NMR relaxation

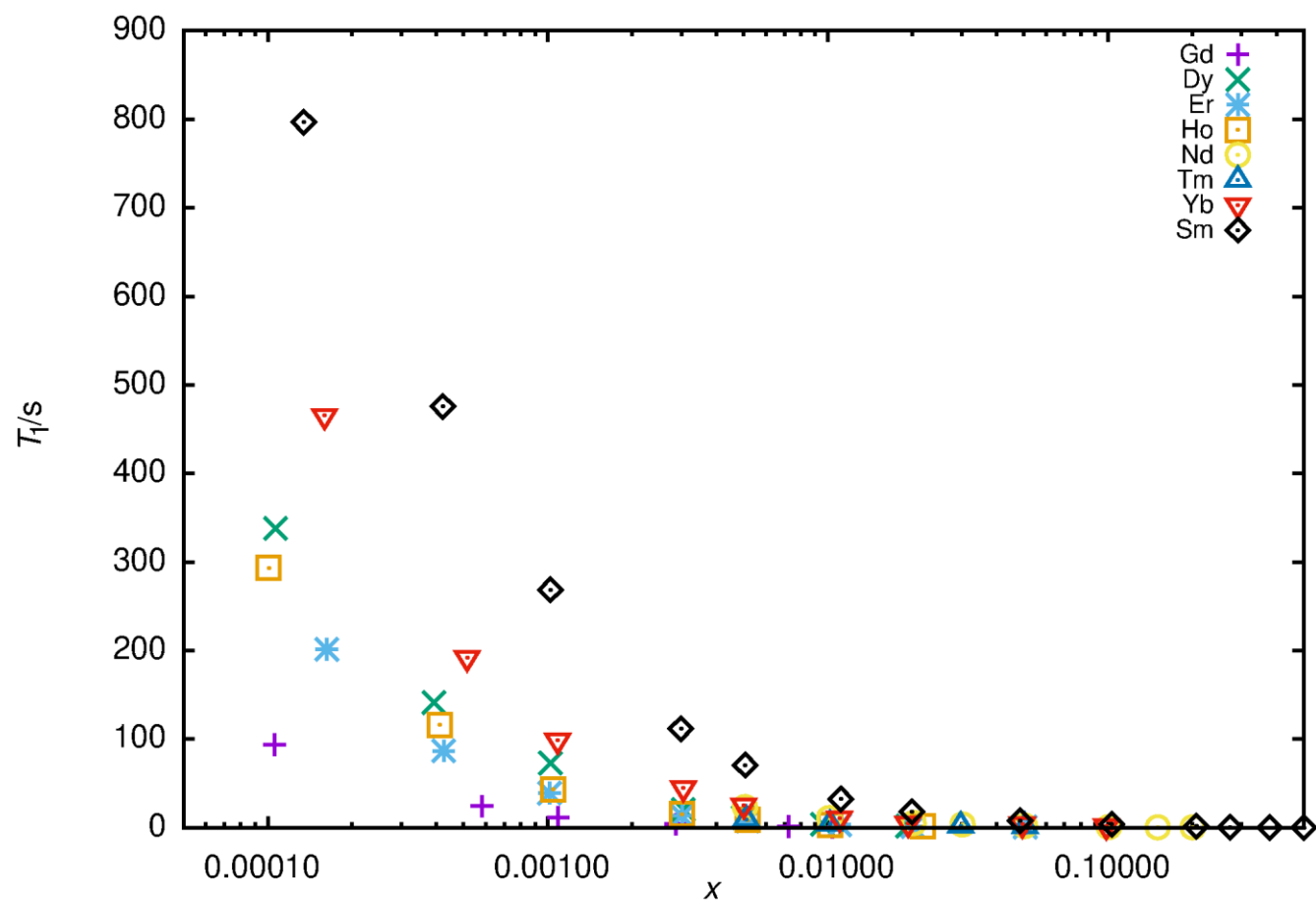


Figure S5: T_1 relaxation data of $\text{LaPO}_4:\text{Ln}$ obtained with the saturation recovery sequence at room temperature in a magnetic field of 9.4 T.

References

- 1 T. Harazono, E. Yokota, H. Uchida and T. Watanabe, *Bull. Chem. Soc. Jpn.*, 1998, **71**, 2797–2805.
- 2 T. Harazono, E. Yokota, H. Uchida and T. Watanabe, *Bull. Chem. Soc. Jpn.*, 1998, **71**, 825–829.
- 3 K. Schmidt-Rohr and H. W. Spiess, *Multidimensional Solid-State NMR and Polymers*, Elsevier, 2012.
- 4 A. J. Pell, G. Pintacuda and C. P. Grey, *Prog. Nucl. Magn. Reson. Spectrosc.* 2019, **111**, 1-271.
- 5 I. Bertini, C. Luchinat, G. Parigi and E. Ravera, *NMR of Paramagnetic Molecules: Applications to Metallobiomolecules and Models*, Elsevier, 2016.
- 6 Y. Ni, J. M. Hughes and A. N. Mariano, *Am. Mineral.*, 1995, **80**, 21–26.
- 7 C. H. Evans, *Biochemistry of the Lanthanides*, Springer Science & Business Media, 2013.